







Ramp Approach Parameter Correction Method for 3-axis Web Machining

Min Zhou¹ , Kang Zhou² , Guolei Zheng³  and Tengfei Li⁴ 

¹China Agricultural University, zhoumin2016@cau.edu.cn,

²Beijing Xuanyu Information Technology Co., Ltd, 806145732@qq.com

³Beihang University, zhengguolei@buaa.edu.cn

⁴Beijing 3D printing research institute, tengfeili333@bcu.edu.cn

Corresponding author: Guolei Zheng, zhengguolei@buaa.edu.cn

Abstract. In 3-axis pocket machining using an insert milling cutter, if the ramp approach parameters are inappropriate, interference usually occurs when the cutter plunges into material. To detect and avoid interference due to inappropriate approach parameters, a ramp approach parameter correction method for web machining is proposed in this study. First, interference-free principles for ramp approach are established. Then, to correct the length and angle of the ramp toolpath, circumscribed circle method and two methods of equal-ratio compression and layer-adding method are proposed respectively. Finally, the correction algorithm is developed and verified by an example. The results show that there is no track of interference during the approach.

Keywords: Approach Interference; Ramp Approach; CNC Machining; Post Processing

DOI: <https://doi.org/10.14733/cadaps.2021.1050-1060>

1 INTRODUCTION

In computer numerical control (CNC) pocket milling, the web features on the bottom surface of a pocket are usually machined by a 3-axis pocketing operation. The basic operation of the processing macro for web pocketing is usually performed by a combination of the axis motion and the ramp motion. If the ramp parameters of the approach macro are inappropriate, interference occurs when machining the pocket with a numerical control (NC) machining program. In NC machining, the process file corresponding to the NC machining program is often missing; thus, it is impossible to intuitively detect the approach interference of the main surface by the current commercial CAM system. As a result, a technician has to use a machining simulation to detect interference and manually calculate the appropriate ramp inflection points one by one, a labor intensive, inefficient process. Therefore, it is necessary to detect and correct the ramp approach parameters automatically for web machining to avoid interference.

A lot of research has been made on interference in NC machining, especially in 5-axis machining. In the review paper by Tang [15], collisions are classified as either local or global. Local collisions include local gouging and rear gouging, which leads to over-cutting of the materials. In the study by Li et al. [11], cutter interference is classified into two types, gouging and collision, where the former is defined in the same way as local collision in reference [15]. Both of these lead low tool life, machining accuracy and surface quality, and even severe equipment damage [8,9]. In addition, they propose an algorithm involving an iterative process of cutter projection to compute the gouge-free cutter positions by the cutter partition method. Zhang et al. [21] model the interference between a tool and a workpiece as the approaching extent evaluation of the tool swept envelope surface and the vibrating workpiece surface in the milling process. They define a metric to quantitatively evaluate the approaching extent and formulate the process parameter planning as a minimax optimization problem.

In the study by Shao et al. [14], a multi-objective evolutionary algorithm is proposed to detect tool interference, which not only avoids the gouge problems resulting from an unsuitable forward step during tool movement, but also ensures that the generated tool path is the interference-free tool path. Wang and Sun [18] use the interference-free spiral milling NC machining tool path to predict and compensate for deformation errors during the spiral milling of blades. Zhang et al. [22] use rational Bézier motion to generate an interference-free tool path for 5-axis sculptured surface machining with a flat-end cutter. A bounding sphere is used as the bounding box to detect the collision by the sweep plane approach in the studies conducted by Tang and Bohez [16,17]. With their method, only the largest collision of each type must be corrected. Kim [7] proposes a safe and shortest tool-setting algorithm using a safe space to avoid holder collision with the workpiece.

Kanda and Morishige [5] calculate machine coordinates and develop a corresponding tool path generation for structural interference among machine components, such as tables, spindles, and columns. Utilizing the idea of admissible area interpolation for the whole designed free-form surface, Lin et al. [12] propose an algorithm to generate the tool posture collision-free area for the free-form surface during the 5-axis CNC finishing period. The tool entry/exit angle is considered in the cutter/workpiece engagement model of the 5-axis ball-end milling in the study by Zhang et al. [23]. In Yu et al.'s paper [25], a novel tool orientation optimization method for 3 + 2-axis machining using a fillet-end cutter based on the sample points selection method and the average strip width estimation method is introduced.

Besides, interference-free tool path for 5-axis CNC machining is studied a lot [1-4,6,10,13,19,20,24]. However, interference avoidance strategies for tool plunging into materials for 3-axis machining has not been studied. This paper focuses on ramp approach parameter correction for 3-axis web machining to avoid interference. The remainder of this paper is organized as follows. First, the main principles for ramp approach parameter correction are established in section 2. In section 3, ramp parameters, including ramp length and ramp angle, are corrected by various techniques. In section 4, the algorithm of the proposed correction method is given and an example is provided to verify the algorithm. Finally, conclusions are presented in section 5.

2 CORRECTION PRINCIPLES OF RAMP APPROACH PARAMETERS

As we know, to avoid cutter damage, ramp, pre-drill and helix are three common approach methods when the cutter entry the stock material. As shown in Figure 1, the green lines represent the ramp approach tool-path. The tool-path is a serials ramp spirals downward straight lines. And it includes three parameters: the rising/falling height h , the ramp angle α , and the ramp length l . Wherein, h is the height of the ramp approach tool-path in the vertical direction; α is the angle between the straight line forming the ramp path and the horizontal plane; and the l is the length of the ramp approach tool-path projected on the horizontal plane. When the ramp length l is small, a part of the material cannot be completely cut off. As a result, when the material is piled up to a certain height, the non-cutting edge of the tool would participate in the cutting, which could damage the cutter. Besides, the web of the bottom surface of the pocket is usually machined by a

large-diameter insert cutter. Because the large-diameter insert milling cutter is not full-tooth at the bottom, the non-tooth part does not contribute to the cutting. Thus, the ramp angle should be appropriate to avoid cutter damage. Therefore, appropriate parameter ranges are proposed first.

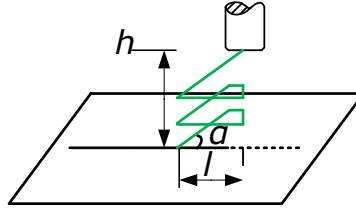


Figure 1: Schematic diagram of the ramp approach.

2.1 Principle for the Ramp Length

As shown in Figure 2, the solid line represents the tool state at the start position of the ramp, *abc* is the area to be machined by the inner edge of the insert milling cutter, and the dotted line represents the tool state at the end position of the ramp. If the ramp length *l* in the horizontal direction is small, then region *abc* is not completely removed by the inner edge of the tool. Area *cde* (the red region in Figure 2) represents the residual region. As can be seen from Figure 2, when *d* and *c* coincide, there is no residual area. Thus, the minimum ramp length *l_{min}* should satisfy $l_{min} = D - 2r$. Thus, the principle for ramp length is:

$$l \geq l_{min} \tag{1}$$

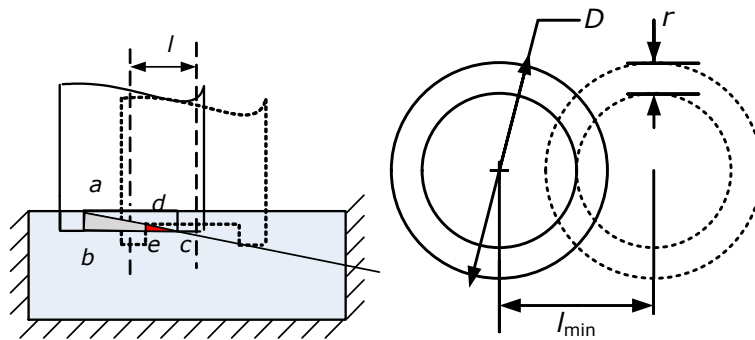


Figure 2: Selection of ramp length in horizontal direction.

2.2 Principle for the Ramp Angle

As shown in Figure 3, the critical ramp angle α_{lim} should satisfy $\alpha_{lim} = \arctan (h_{ic} / l_{nc})$, where h_{ic} is the cutting height in the tool; and l_{nc} is the length of the non-cutting section at the bottom of the tool. Here, $l_{nc} = D - 2r$, where *D* and *r* are the diameter and the bottom circle radius of the insert milling cutter, respectively.

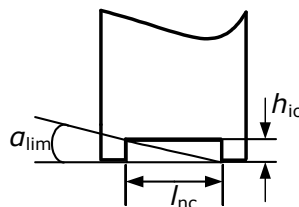


Figure 3: Critical ramp angle of the insert milling cutter.

As shown in Figure 4, A_1 is a material body that can be cut by a tool, and A_2 is a material body that needs to be removed in the entire cavity. When $a > a_{lim}$, part of the non-cutting edge on the bottom of the tool participates in the cutting and damages the tool, as shown by the red line segment in Figure 4. Therefore, the ramp angle a should satisfy the inequality $a \leq a_{lim}$ to ensure that the non-cutting edge of the insert tool does not participate during the cutting to avoid tool damage. That is,

$$a \leq \arctan (h_{ic} / l_{nc}) \tag{2}$$

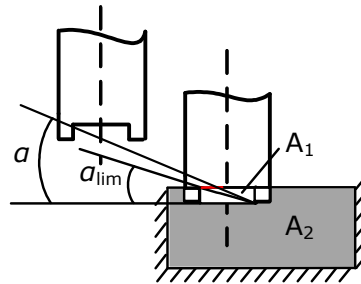


Figure 4: Non-cutting edge participating during cutting.

3 CORRECTION OF RAMP APPROACH PARAMETERS

3.1 Ramp Length Correction

To correct the ramp length, a circumscribed circle method is proposed. As shown in Figure 5, the projection of the ramp approach section on the XOY plane in the machine coordinate system is $P_1 \rightarrow P_2 \rightarrow P_3 \rightarrow \dots \rightarrow P_n$, i.e., a total of $n - 1$ line segments. The length of the line segment between the adjacent two points is called the ramp length l .

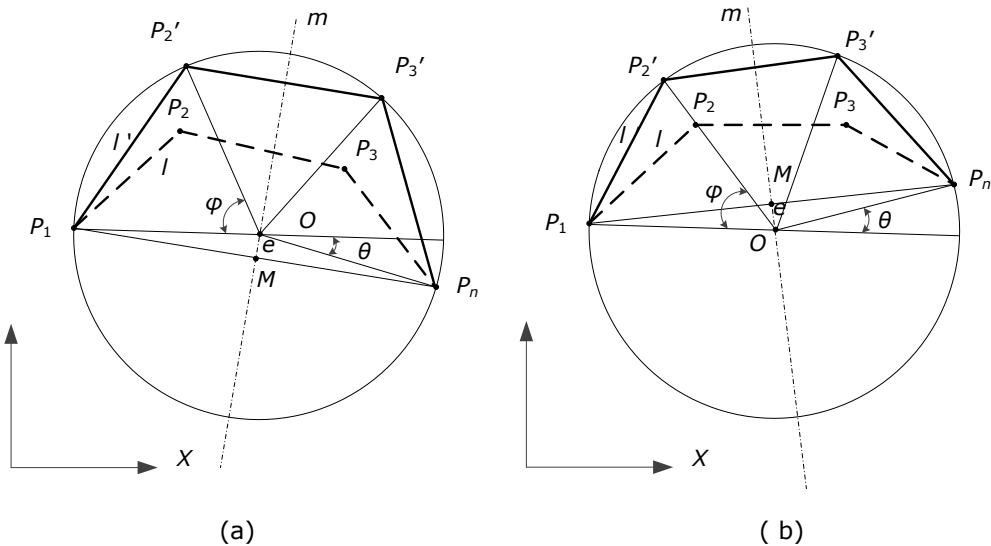


Figure 5: Semantic diagram of ramp length correction: (a) O and the endpoints are on the same side, and (b) O and the endpoints are on different sides.

Make a mid-perpendicular line m pass through the midpoint M of line segment P_1P_n . Take a point O on the mid-perpendicular line m and ensure that O and the points P_2, P_3, \dots, P_{n-1} are on the same side of the line segment P_1P_n . Make an auxiliary circle with O as the center and OP_1 as the radius.

Next, divide the superior arc P_1P_n into $n - 1$ equal parts to obtain the corrected projection $P_1 \rightarrow P_2' \rightarrow P_3' \rightarrow \dots \rightarrow P_n$ of the polyline. Let the optimized ramp length be l' , where l' satisfies $l' \geq l_{\min}$; the polyline corresponding to the projection with $P_1 \rightarrow P_2' \rightarrow P_3' \rightarrow \dots \rightarrow P_n$ as end points is the approach section that satisfies Eq. (1). The calculation formula is

$$180^\circ + \theta = (n - 1) \varphi$$

where $\tan \frac{\theta}{2} = \frac{e}{0.5s} (-\frac{\pi}{2} \leq \frac{\theta}{2} \leq \frac{\pi}{2})$; $\sin \frac{\varphi}{2} = \frac{0.5l'}{R} (-\frac{\pi}{2} \leq \frac{\varphi}{2} \leq \frac{\pi}{2})$; $R = \sqrt{\frac{1}{4}s^2 + e^2}$; e is the distance between O and M ; s is the length of the line segment P_1P_n ; φ is the arc angle corresponding to each arc after the superior arc P_1P_n is equally divided; and θ is the angle between the extension line of P_1O and OP_n . The relation between l' and e can be obtained as

$$\begin{aligned} \theta &= 2 \arctan \frac{2e}{s} \\ \varphi &= 2 \arcsin \frac{l'}{\sqrt{s^2 + 4e^2}} \\ 90^\circ + \arctan \frac{2e}{s} &= (n - 1) \arcsin \frac{l'}{\sqrt{s^2 + 4e^2}} \end{aligned}$$

By selecting the appropriate e , l' can satisfy $l' \geq l_{\min}$.

When point O , which is on the vertical line m , is on the other side of the line segment P_1P_n , that is, O and the points P_2, P_3, \dots, P_{n-1} are not on the same side, as shown in Figure 5(b), then the calculation formula is

$$180^\circ - \theta = (n - 1) \varphi$$

Where θ and R have the same definitions as above except φ . φ is the arc angle corresponding to each arc after the inferior arc P_1P_n is equally divided. Next, the relation between l' and e can be obtained as

$$\begin{aligned} \theta &= 2 \arctan \frac{2e}{s} \\ \varphi &= 2 \arcsin \frac{l'}{\sqrt{s^2 + 4e^2}} \\ 90^\circ - \arctan \frac{2e}{s} &= (n - 1) \arcsin \frac{l'}{\sqrt{s^2 + 4e^2}} \end{aligned}$$

By selecting the appropriate e , l' can satisfy $l' \geq l_{\min}$.

After obtaining the projection of the corrected ramp tool-path, the optimization result of ramp length can be obtained according to the X and Y coordinates of endpoints $P_2', P_3', \dots, P_{n-1}'$.

3.2 Ramp Angle Correction

To correct the ramp angle, the equal-ratio compression method and the layer-adding method are proposed. The former is based on engineering experience and the latter is a method of deriving correction parameters in reverse based on the target results.

3.2.1 Equal-ratio compression method

To make the new ramp angle $a' < a$, the height of the ramp inflection point of the approach section is reduced by compression, while the rest of the data is unchanged. This method is called the equal-ratio compression method. Taking the main surface of the web as the reference surface, the ratio of the new position height to the original position height, denoted by ν , is called the compression ratio.

As shown in Figure 6, P_2 is the start ramp point, and P_5 is the end ramp point, $h_1 = z_2 - z_5$, $h_2 = z_3 - z_5$, $h_3 = z_4 - z_5$. Taking the main surface of the web as the reference surface, the optimized

position height $h_1' = A_p + 2 \sim 3$ mm and the compression ratio $v = h_1' / h_1$, where A_p is the maximum depth of cut for the pocket machining; and $2 \sim 3$ mm is an experience value. Lower the start ramp point P_2 to the height position of h_1' obtaining P_2' (x_2', y_2', z_2'), where $z_2' = z_2 + h_1'$. The remaining endpoints are sequentially compressed at compression rate v except the end point. During the compression process, for the new ramp angle a' to satisfy $\tan a' = v \tan a$ and to further obtain the optimized ramp tool-path, only the z-coordinate is multiplied by the compression ratio, while the x-coordinate and y-coordinate are unchanged. After the equal-ratio compression, if the optimized a' does not satisfy inequality (2), the layer-adding method is adopted to solve the ramp angle parameter correction problem.

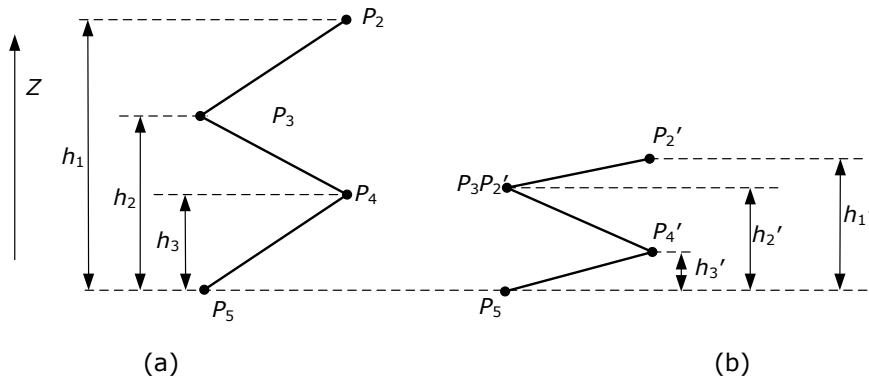


Figure 6: Schematic diagram of equal-ratio compression method: (a) Before correction, and (b) After correction.

3.2.2 Layer-adding method

To make the new ramp angle $a' < a$, the method of increasing the number of ramp layers and performing equal-ratio compression is called the layer-adding method. The ratio of the number of corrected ramp layers to the number of the original ramp layers is called the layer-adding rate, which is represented by w . As can be seen from the definition of the layer-adding method, the layer-adding method includes the principle of equal-ratio compression. Using the layer-adding method, an appropriate ramp angle a' ($a' \leq a_{lim}$) is first calculated. Next, the layer-adding rate is derived inversely according to the compression ratio v ($v = \frac{\tan a'}{\tan a}$). Finally, the machine position coordinates corresponding to the new ramp tool-path are calculated.

Firstly, the ramp tool-path is projected onto the XOY horizontal plane. According to whether the projection trajectory is closed, the layer-adding type is divided into unidirectional layering and bidirectional layering. As shown in Figure 7(a), if the projection trajectory is closed, that is, when the x and y coordinates of the start point and the end point of the ramp tool-path are the same, unidirectional layering is adopted. If the projection trajectory is open, that is, when the projections of the start point and the end point do not coincide, the bidirectional layering method is applied, as shown in Figure 7(b), where the direction of the arrow is the direction of the layer-adding.

Set the original ramp height to h ; then $h' = v * h$ is the height compressed by the compression ratio v . If the unidirectional layering method is adopted, the layer-adding ratio is $\omega = \lceil \Delta h / h' \rceil = \lceil (1-v)/v \rceil$. If the bidirectional layering method is applied, the layer-adding ratio is $\omega = \lceil \Delta h / h' \rceil = \lceil (1-v)/(2v) \rceil$, where the symbol $\lceil \cdot \rceil$ means to round up to the nearest integer.

Taking the bidirectional layering as an example, the black thick solid line segments $P_2P_3P_4P_5$ in Figure 7(c) show the original ramp approach section. Given an appropriate ramp angle α' ($\alpha' \leq \alpha_{lim}$), the ramp tool-path is compressed by the compression ratio $v = \frac{\tan \alpha'}{\tan \alpha}$ to obtain the line segments $P_2'P_3'P_4'P_5$ shown by the green line. Line segments $P_2'P_3'P_4'P_5$ are layer-added by the layer-adding ratio $w = [\Delta h/h'] = [(1-v)/(2v)]$. The different layers are connected by means of the original path back. As a result, the optimized ramp angle by the layering method can be obtained as shown by the green line segments in Figure 8c, where the layer-adding ratio is $w = 3$, and the compression ratio is $v = 1/7$.

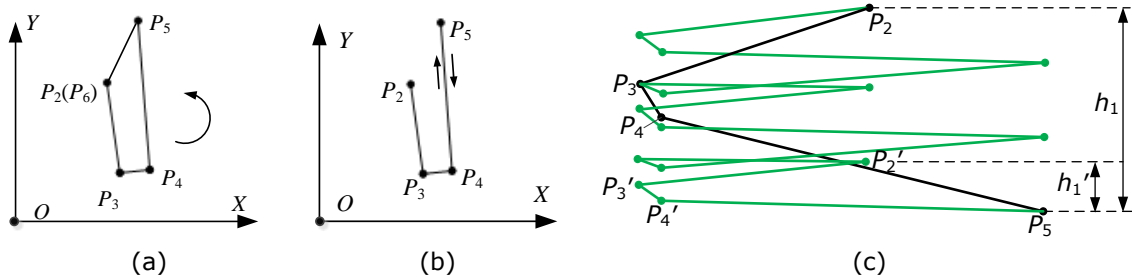


Figure 7: Layer-adding method: (a) Unidirectional layering, (b) Bidirectional layering, and (c) Example of bidirectional layering.

Because the equal-ratio compression method is based on engineering experience, sometimes the optimized result may not satisfy inequality (2). However, since it does not increase the number of the cutter positions, as the layer-adding method does, the equal-ratio compression method is selected first. If the optimized result using the equal-ratio compression method is not appropriate, then the layer-adding method is the alternative solution.

4 ALGORITHM AND EXAMPLE

The algorithm for parameter correction in the ramp approach is provided in Figure 8. The detailed steps are as follows.

Step 1: Extract the tool machine motion trajectory according to the input NC machining program.

Step 2: Recognize the ramp approach section.

Step 3: Determine whether the ramp length is appropriate. If the ramp length l does not satisfy inequality (1), then go to Step 4; if the ramp length l satisfies inequality (1), then go directly to Step 5.

Step 4: Correct the ramp length. Go to Step 5.

Step 5: Determine whether the ramp angle meets inequality (2). If the ramp angle α is less than or equal to the critical ramp angle α_{lim} , then go to the end; if $\alpha > \alpha_{lim}$, then go to Step 6.

Step 6: Optimize the ramp angle using the equal-ratio compression method. Go to Step 7.

Step 7: Determine whether the ramp angle meets inequality (2). If the ramp angle α is less than or equal to the critical ramp angle α_{lim} , then go to Step 9; if $\alpha > \alpha_{lim}$, then go to Step 8.

Step 8: Correct the original ramp angle α with the layer-adding method. Go to Step 9.

Step 9: Modify the NC program according to the corrected ramp tool-path. Go to the end.

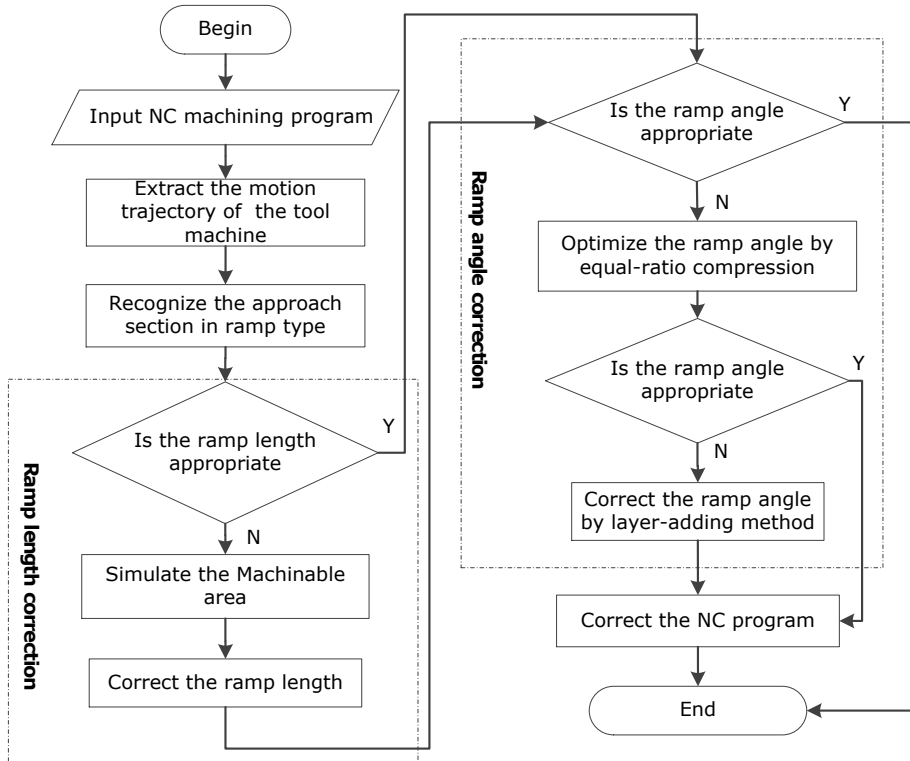


Figure 8: Flowchart of ramp approach parameter correction algorithm.

To validate the effectiveness of the proposed approach, the presented algorithm has been tried on several parts and one example of them is given in this paper as shown in Figure 9. In this example, the bottom surface of the pocket shown in Figure 9a is rough machined by the insert milling cutter with four layers because the depth of the pocket is large. Therefore, the ramp approach is employed four times. As shown in Figure 9b, the red lines illustrate the original ramp approach tool-path for the four layers as input, and the four ramp angles are all larger than the preset value of 3° . The bad ramp angles would lead approach interference. The equal-compression method is adopted to correct the ramp angles first. However, as the green lines shown in Figure 9b, only the optimized ramp angle for the first layer satisfies inequality (2), the ramp angles of the 2nd, 3rd, and 4th approach sections are too large to be corrected by the equal-compression method. Thus, the layer-adding correction method is adopted. Figure 10c shows the correction result of ramp tool-path for the 2nd layer using the unidirectional layering method. Wherein, the yellow lines are the original tool-path while the green lines are the corrected ramp approach tool-path. Finally, the correction NC machining program is simulated on a VERICUT (CGTech, Irvine, CA, US) without interference. Therefore, our algorithm operated effectively and reliably on the test cases.

5 CONCLUSION

To solve the interference problem caused by inappropriate ramp approach parameters when the cutter plunges into material, principles of the interference-free of the ramp approach by the insert milling cutter is proposed in this study. The ramp approach tool-path includes two important parameters: the ramp angle α and the ramp length l . For the ramp length, the circumscribed circle technique is proposed to detect and correct it. To correct the ramp angle, two methods of equal-ratio compression and layer-adding for ramp angle correction are proposed. The experiment result

shows that there's no interference in the 3-axis web machining by the addressed techniques. And the algorithm is effective for the tested examples.

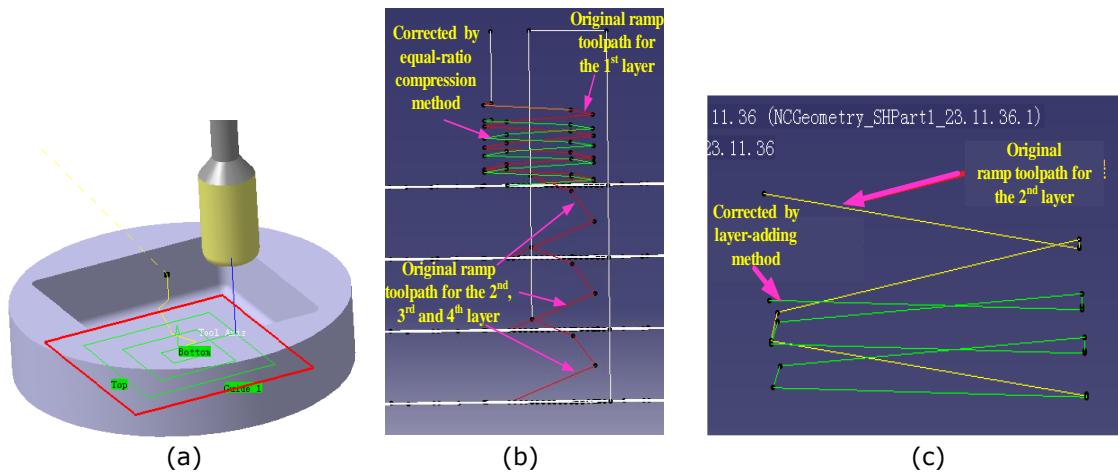


Figure 9: Implementation example: (a) Part, (b) correction result by equal-compression method for the 1st layer, and (c) correction result by layer-adding method for the 2nd layer.

In the ramp angle correction, there is no better method to predict whether the equal-ratio compression method is appropriate but the trial-and-error method. Besides, the test examples are not enough. These are the limitations of the study. Our further research will focus on to solve the problems as much as possible.

ACKNOWLEDGEMENT

This research was supported by the Shanghai Aerospace Science and Technology Innovation Fund under Grant No. SAST2019-124 and China Agricultural University's counterpart support research cooperation fund under Grant No. 2020SF003.

Min Zhou, <https://orcid.org/0000-0002-8569-5846>

Kang Zhou, <https://orcid.org/0000-0002-4078-8096>

Guolei Zheng, <https://orcid.org/0000-0002-3887-6265>

Thengfei, Li, <https://orcid.org/0000-0002-5907-8043>

REFERENCES

- [1] Bo, P.; Bartoň, M.; Pottmann, H.: Automatic fitting of conical envelopes to free-form surfaces for flank CNC machining, *Computer-Aided Design*, 91, 2017, 84-94. <https://doi:10.1016/j.cad.2017.06.006>
- [2] Calleja, A.; Bo, P.; González Haizea; Bartoň, M.; López de Lacalle Luis Norberto: Highly accurate 5-axis flank CNC machining with conical tools, *The International Journal of Advanced Manufacturing Technology*, 97(5-8), 2018, 1605-1615. <https://doi:10.1007/s00170-018-2033-7>
- [3] Chiou, C.J.; Lee, Y. S.: A machining potential field approach to toolpath generation for multi-axis sculptured surface machining, *Computer-Aided Desig*, 34(5), 2002, 357-71. [https://doi:10.1016/S0010-4485\(01\)00102-6](https://doi:10.1016/S0010-4485(01)00102-6)

- [4] Geng, C.; Yu, D.; Zheng, L.; Zhang, H.; Wang, F.: A tool path correction and compression algorithm for five-axis CNC machining, *Journal of Systems Science and Complexity*, 26(5), 2013, 799-816. <https://doi:10.1007/s11424-013-3101-6>
- [5] Kanda, T.; Morishige, K.: Tool Path Generation for Five-Axis Controlled Machining with Consideration of Structure Interference, *International Journal of Automation Technology*, 6(6), 2012, 710-716. <https://doi:10.20965/ijat.2012.p0710>
- [6] Kim, Y. J.; Elber, G.; Bartoň, M.; Pottmann, H.: Precise gouging-free tool orientations for 5-axis CNC machining, *Computer-Aided Design*, 58, 2015, 220-229. <https://doi:10.1016/j.cad.2014.08.010>
- [7] Kim, S. J.: Short and safe tool setting by safe space in NC machining, *The International Journal of Advanced Manufacturing Technology*, 33(9-10), 2007, 1017-1023. <https://doi:10.1007/s00170-006-0526-2>
- [8] Lee, Y. S.: Admissible tool orientation control of gouging avoidance for 5-axis complex surface machining, *Computer-Aided Design* 29(7), 1997, 507-521. [https://doi:10.1016/S0010-4485\(97\)00002-X](https://doi:10.1016/S0010-4485(97)00002-X)
- [9] Lee, Y. S.; Chang, T. C.: 2-phase approach to global tool interference avoidance in 5-axis machining, *Computer-Aided Design*, 27(10), 1995, 715-729. [https://doi:10.1016/0010-4485\(94\)00021-5](https://doi:10.1016/0010-4485(94)00021-5)
- [10] Lee, Y. S.: Admissible tool orientation control of gouging avoidance for 5-axis complex surface machining, *Computer-Aided Design*, 29(7), 1997, 507-21. [https://doi:10.1016/S0010-4485\(97\)00002-X](https://doi:10.1016/S0010-4485(97)00002-X)
- [11] Li, X. Y.; Lee, C. H.; Hu, P. C.; Zhang, Y.; Yang, F. Z.: Cutter partition-based tool orientation optimization for gouge avoidance in five-axis machining, *The International Journal of Advanced Manufacturing Technology*, 95(5-8), 2018, 2041-2057. <https://doi:10.1007/s00170-017-1263-4>
- [12] Lin, Z. W.; Sheng, H. Y.; Gan, W. F.; Fu, J. Z.: Approximate tool posture collision-free area generation for five-axis CNC finishing process using admissible area interpolation, *The International Journal of Advanced Manufacturing Technology*, 62(9-12), 2012, 1191-1203. <https://doi:10.1007/s00170-011-3851-z>
- [13] Rao, A.; Sarma, R.: On local gouging in five-axis sculptured surface machining using flat-end tools, *Computer Aided Design*, 32, 2000, 409-420. [https://doi:10.1016/S0010-4485\(99\)00105-0](https://doi:10.1016/S0010-4485(99)00105-0)
- [14] Shao, Z.; Guo, R.; Li, J.; Peng, J.: Study on algorithm for interference-free tool path generation of free-form surfaces based on Z-map model, 9th International Conference on Electronic Measurement & Instruments, 2009, 4-1005-4-1010. <https://doi:10.1109/ICEMI.2009.5274147>
- [15] Tang, T. D.: Algorithms for collision detection and avoidance for five-axis NC machining: a state of the art review, *Computer-Aided Design*, 51, 2014, 1-17. <https://doi:10.1016/j.cad.2014.02.001>
- [16] Tang, T. D.; Bohez, E. L. J. Bohez: A new collision avoidance strategy and its integration with collision detection for five-axis NC machining, *The International Journal of Advanced Manufacturing Technology*, 81(5-8), 2015, 1247-1258. <https://doi:10.1007/s00170-015-7293-x>
- [17] Tang, T. D.; Bohez, E. L. J.; Koomsap, P.: The sweep plane algorithm for global collision detection with workpiece geometry update for five-axis NC machining, *Computer-Aided Design*, 39(11), 2007, 1012-1024. <https://doi:10.1016/j.cad.2007.06.004>
- [18] Wang, M. H.; Sun, Y.: Error prediction and compensation based on interference-free tool paths in blade milling, *The International Journal of Advanced Manufacturing Technology*, 71(5-8), 2014, 1309-1318. <https://doi:10.1007/s00170-013-5535-3>
- [19] Wang, Q. H.; Li, J. R.; Gong, H. Q.: Graphics-assisted cutter orientation correction for collision-free five-axis machining, *International journal of production research*, 45(13), 2007, 2875-2894. <https://doi:10.1080/00207540600767798>

- [20] Xie, L.; Ruan, X. Y.; Li, M.; Wu, Q. J.: Interference-Free Tool Path Generation for 5-Axis NC Machining with a Flat-End Cutter, *Key Engineering Materials*, 315, 2006, 180-184. <https://doi:10.4028/www.scientific.net/KEM.315-316.180>
- [21] Zhang, X. M.; Zhang, D.; Cao, L.; Huang, T.; Zhang, J.; Ding, H.: Minimax Optimization Strategy for Process Parameters Planning: Toward Interference-Free Between Tool and Flexible Workpiece in Milling Process, *Journal of Manufacturing Science and Engineering*, 139(5), 2017, 051010. [https://doi: 10.1115/1.4035184](https://doi:10.1115/1.4035184)
- [22] Zhang, W.; Zhang, Y. F.; Ge, Q. J.: Interference-free tool path generation for 5-axis sculptured surface machining using rational Bézier motions of a flat-end cutter, *International Journal of Production Research*, 43(19), 2005, 4103-4124. <https://doi:10.1080/00207540500168188>
- [23] Zhang, X.; Zhang J.; Zheng, X.; Pang, B.; Zhao, W.: Tool orientation optimization of 5-axis ball-end milling based on an accurate cutter/workpiece engagement mode, *CIRP Journal of Manufacturing Science and Technology*, 19, 2017, 106-116. <https://doi:10.1016/j.cirpj.2017.06.003>
- [24] Zheng, G.; Zhu, L.; Bi, Q.: Cutter size optimization and interference-free tool path generation for five-axis flank milling of centrifugal impellers, *International Journal of Production Research*, 50(23), 2012, 6667-6678. <https://doi:10.1080/00207543.2011.611631>
- [25] Zhu, Y.; Chen, Z. T.; Ning, T.; Xu, R. F.: Tool orientation optimization for 3+ 2-axis CNC machining of sculptured surface, *Computer-Aided Design*, 77, 2016, 60-72. <https://doi:10.1016/j.cad.2016.02.007>